1954

Local buckling of wide flange shapes - to crc -, 1954

G. Haaijer

B. Thurlimann

Welded Continuous Frames and Their Components

Status Report on Project 205E (Inelastic Instability)

Local Buckling of Wide-Flange Shapes

by

Geerhard Haaijer and Bruno Thürlimann

(Not for Publication)

Prepared for Annual Meeting of Committee C of Column Research Council, May 27, 1954

This work has been carried out as a part of an investigation sponsored jointly by the Welding Research Council and the Department of the Navy with funds furnished by the following:

American Institute of Steel Construction
American Iron and Steel Institute
Institute of Research, Lehigh University
Column Research Council (Advisory)
Office of Naval Research (Contract No. 39303)
Bureau of Ships
Bureau of Yards and Docks

Fritz Engineering Laboratory
Department of Civil Engineering & Mechanics
Lehigh University
Bethlehem, Pennsylvania

May 21, 1954

Fritz Laboratory Report No. 205E.4

I. Introduction

In order to solve the problem of buckling of a plate, the relationships between additional stresses and strains due to the deflection of the plate out of its plane have to be known.

In the elastic range the assumption that the material is isotropic and homogeneous leads to solutions which are in very good agreement with test-results.

Several investigators have given theoretical solutions for buckling in the plastic range based on different stress-strain relationships. The discrepancies between the different theories are basically due to these stress-strain relationships, which by some authors are directly assumed and by others are derived for materials with idealized behavior.

It is the purpose of the local buckling project at Lehigh University to arrive at a solution of this problem which will apply to structural steel plates. Ultimately the aim is to specify the dimensions of rolled shapes in such a way that they can sustain sufficiently large deformations without occurance of local buckling.

In the following theoretical considerations the stress-strain relationships have been kept quite general. Comparison of test results with the solutions obtained in this way will give some indications of the value of the different variables involved.

As long as no other information from direct tests with regard to the stress-strain relationships is available, this seems to be the only way to arrive at a practical solution of the problem.

2. Stress-Strain Relationships

Consider a plate made out of a material exhibiting a stress-strain curve in simple tension as shown in Figure 2.1. The notation subsequently used is given in this same Figure.

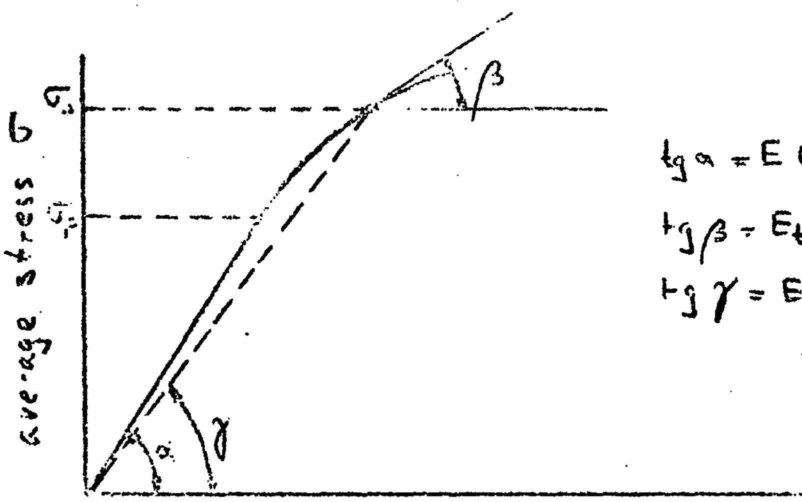

Fig. 2.1

Take the center plane of the plate as the x-y coordinate plane. Compressing the plate in the x-direction into the plastic range up to a stress σ_o may affect all the deformation properties. Hence the tangent moduli in the x-and y-direction are possibly different. The same may hold for Poisson's ratios in the x- and y- direction. The shearing modulus may also be affected.

Call

$$\frac{\partial \varepsilon_x}{\partial \sigma_x} = \frac{1}{E_{tx}} , \quad \frac{\partial \varepsilon_y}{\partial \sigma_y} = \frac{1}{E_{ty}}$$

$$\frac{\partial \varepsilon_x}{\partial \sigma_y} = -\frac{\nu_y}{E_{ty}} , \quad \frac{\partial \varepsilon_y}{\partial \sigma_x} = -\frac{\nu_x}{E_{tx}} \qquad (2.1)$$

$$\frac{\partial \gamma_{xy}}{\partial \tau_{xy}} = \frac{1}{G_t}$$

The assumption is made that no unloading occurs. Then the relationships between the increments of stress and strain after the material has been compressed in the x direction up to a stress σ_o can be written as

$$d\varepsilon_x = \frac{1}{E_{tx}} d\sigma_x - \frac{\nu_y}{E_{ty}} d\sigma_y$$

$$d\varepsilon_y = -\frac{\nu_x}{E_{tx}} d\sigma_x + \frac{1}{E_{ty}} d\sigma_y \qquad (2.2)$$

$$d\gamma_{xy} = \frac{1}{G_t} d\tau_{xy}$$

Or with stresses in terms of strains

$$d\sigma_x = \frac{E_{tx}}{1-\nu_x\nu_y}\left(d\varepsilon_x + \nu_y d\varepsilon_y\right)$$

$$d\sigma_y = \frac{E_{ty}}{1-\nu_x\nu_y}\left(\nu_x d\varepsilon_x + d\varepsilon_y\right) \qquad (2.3)$$

$$d\tau_{xy} = G_t d\gamma_{xy}$$

In words these relationships state that when uniaxially compressed into the inelastic range the originally isotropic material becomes orthogonal anistropic.

For the case of unloading the material would again behave elastically, but it is now generally agreed ~~be~~, that under test conditions no unloading occurs when a plate starts to buckle.

In table I a summary of the assumed or derived values of E_{tx}, E_{ty}, ν_x, ν_y and G_t as used in different plate buckling theories is given. The variations are quite astonishing.

Due to the inhomogeneous yielding process of steel this material presents an additional problem. A typical stress-strain curve is shown in Figure 2.2.

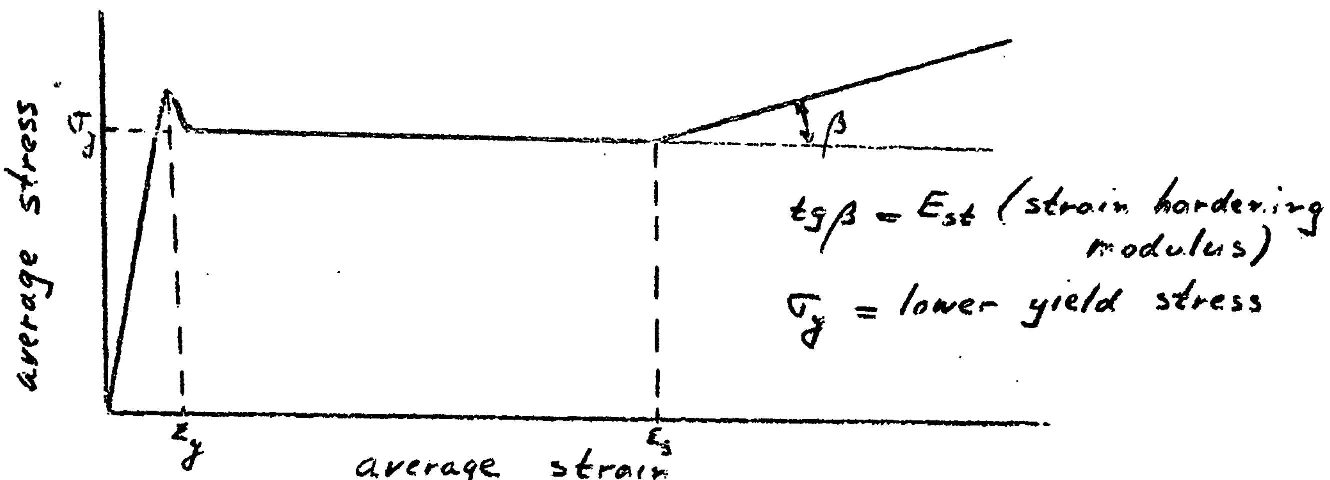

Fig. 2.2

As already emphasized in Progress Report T (Ref. 1) yielding occurs in so called slip bands and the strain "jumps" from ε_y to ε_s. Therefore, as long as the average strain is in between ε_y and ε_s the material will be partly strained up to ε_y and partly up to ε_s: the material is inhomogeneous. Tests have shown that this yielding process is very erratic (Progress Report T).

For the rotation of a plastic hinge it is in general desirable that the average strain in the flanges of a WF shape reaches the strain hardening range (ε average $\geq \varepsilon_s$). Then the material is again more or less homogeneous and only this case will be considered in the following derivations.

Once a satisfactory solution for the strain hardening range is obtained solutions for the intermediate range ($\varepsilon_y < \varepsilon_{av} < \varepsilon_s$) can be derived in a way outlined in Progress Report T.

3. General Stress-Strain Relations Applied to Buckling of Plates

When a plate is loaded by forces acting in its center plane a state of stress and strain may be reached such that besides the plane position also a bent equilibrium position becomes possible: the plate buckles.

If the transition from the plane to the bent position would occur under constant loads, unloading on the convex side of the plate would be inevitable. However, under test conditions buckling occurs with an increase of strain such that no strain reversal takes place.

Shanley proved that the same happens in the case of axially loaded columns. Agreement between his theory applied to rectangular steel columns, which buckled in the strain-hardening range, and test results was shown in Progress Report S (Ref. 2).

Consider again a plate uniformly compressed in the x direction up to a stress σ_o causing orthogonal anisotropy. Calling the deflection perpendicular to the center plane W the expressions for the bending and twisting moments become

$$M_x = -\frac{E_{tx} I}{1-\nu_x\nu_y}\left(\frac{\partial^2 w}{\partial x^2} + \nu_y \frac{\partial^2 w}{\partial y^2}\right)$$

$$M_y = -\frac{E_{ty} I}{1-\nu_x\nu_y}\left(\frac{\partial^2 w}{\partial y^2} + \nu_x \frac{\partial^2 w}{\partial x^2}\right) \qquad (3.1)$$

$$M_{xy} = -2G_t I \frac{\partial^2 w}{\partial x \partial y}$$

with $I = 1/12\, t^3$

t = thickness of plate

The condition that the bent position is an equilibrium position can be expressed by the following differential equation

$$D_x \frac{\partial^4 w}{\partial x^4} + 2H\frac{\partial^4 w}{\partial x^2 \partial y^2} + D_y \frac{\partial^4 w}{\partial y^4} = t\,\sigma_x \frac{\partial^2 w}{\partial x^2} \qquad (3.2)$$

$$D_x = \frac{E_{tx} I}{1-\nu_x\nu_y}$$

$$D_y = \frac{E_{ty} I}{1-\nu_x\nu_y}$$

$$2H = \nu_y D_x + \nu_x D_y + 4G_t I$$

The derivation of these equations may be found in the pertinent literature (Ref. 3). Only if $H^2 = D_x D_y$, an assumption made by Bleich (Ref. 4), solutions of this differential equation can be easily obtained.

The condition that both the plane and the bent positions are equilibrium positions also can be expressed in terms of work.

The additional work done by the external forces due to bending of the plate must equal the change in strain energy of the plate.

This renders the following integral equation

$$\frac{\sigma_0 t}{I} \iint \left(\frac{\partial w}{\partial x}\right)^2 dx\,dy = \iint \left[\frac{E_{tx}}{1-\nu_x \nu_y}\left(\frac{\partial^2 w}{\partial x^2}\right)^2 + \frac{E_{ty}}{1-\nu_x \nu_y}\left(\frac{\partial^2 w}{\partial y^2}\right)^2 + \frac{\nu_y E_{tx} + \nu_x E_{ty}}{1-\nu_x \nu_y}\left(\frac{\partial^2 w}{\partial x^2}\right)\left(\frac{\partial^2 w}{\partial y^2}\right) + 4 G_t \left(\frac{\partial^2 w}{\partial x \partial y}\right)^2\right] dx\,dy \quad (3.3)$$

When external restraints are provided to the plate the right-hand member of equation (3.3) has to be supplemented by additional terms expressing the work done by these restraints.

By assuming an appropriate deflection surface equation (3.3) gives an approximate solution. The degree of approximation depends on the correctness of the assumed deflection surface. In any case the result will be on the upper side.

4. Application of Energy Method to Different Cases of Buckling of Uniformly Compressed Plates

I. Rectangular plate with the loaded edges $x = 0$ and $x = \ell$ hinged, the unloaded edge $y = 0$ restrained against rotation and the unloaded edge $y = b$ free (Fig. 4.1)

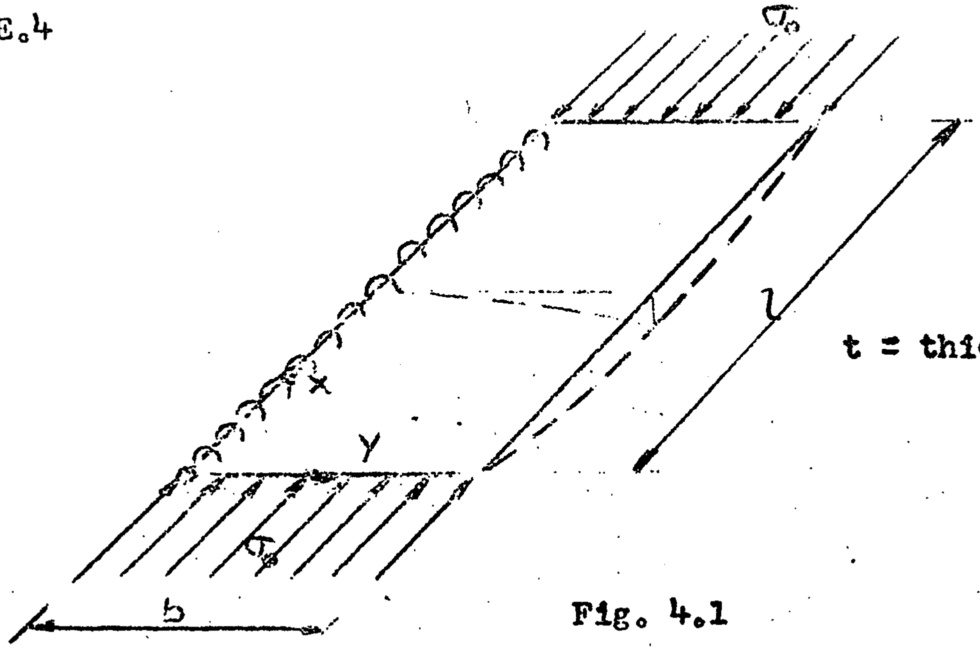

t = thickness of plate

Fig. 4.1

In their paper on buckling of outstanding flanges Lundquist and Stowell (Ref. 5) assumed the following deflection surface, which is known to be good in the elastic range.

$$w = \left[A\frac{y}{b} + B\left\{\left(\frac{y}{b}\right)^2 + a_1\left(\frac{y}{b}\right)^3 + a_2\left(\frac{y}{b}\right)^4 + a_3\left(\frac{y}{b}\right)^5\right\}\right]\sin\frac{\pi x}{\ell} \quad (4.1)$$

with $a_1 = -1.0076$

$a_2 = +0.5076$

$a_3 = -0.1023$

The ratio B/A depends on the amount of restraint. In the case of elastic restraint with ψ = moment per unit length required for a unit rotation

$$\frac{B}{A} = \frac{\psi b}{2 D_y}$$

a. Edge y = o is hinged (B = o)

Substituting w in the energy equation and performing the integration gives

$$\sigma_{cr} = \left(\frac{t}{b}\right)^2\left[\frac{\pi^2 E_{tx}}{12(1-\nu_x\nu_y)}\left(\frac{b}{\ell}\right)^2 + G_t\right] \quad (4.3)$$

For a long plate the first term can be neglected and

$$\sigma_{cr} = \left(\frac{t}{b}\right)^2 G_t \quad (4.4)$$

b. Edge y = o is completely fixed (A = o)

The minimum value of σ_{cr} is obtained when the half-wave length l satisfies

$$\frac{l}{b} = 1.646\sqrt[4]{\frac{E_{tx}}{E_{ty}}} \quad --- \quad (4.5)$$

Then

$$\sigma_{cr} = \left(\frac{t}{b}\right)^2 \left[\frac{7.275\sqrt{E_{tx}E_{ty}} - 0.506(\nu_y E_{tx} - \nu_x E_{ty})}{12(1-\nu_x\nu_y)} + 1.371\, G_t\right] \quad (4.6)$$

II. Rectangular plate with the loaded edges hinged, the unloaded edges having equal restraint against rotation (Fig. 4.2)

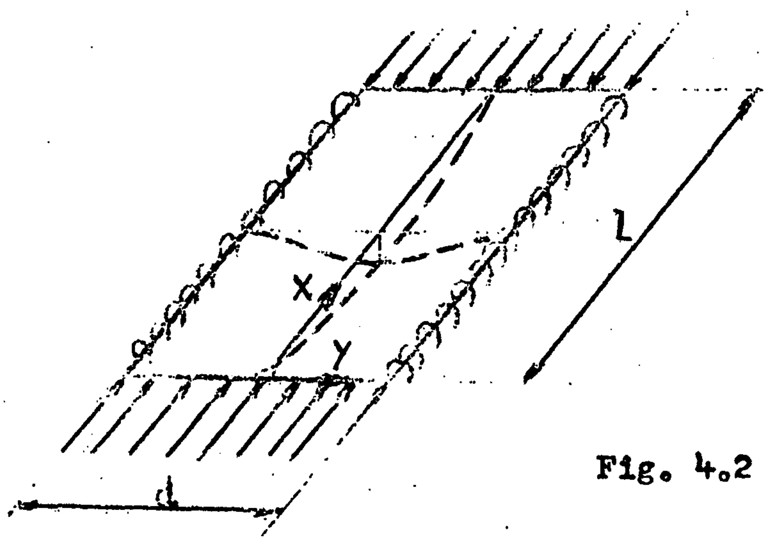

w = Thickness of plate

Fig. 4.2

For this case the following deflection surface is used (see Ref. 6)

$$w = \left[B\pi\left(\frac{y^2}{d^2} - \frac{1}{4}\right) + (A+B)\cos\frac{\pi y}{d}\right]\sin\frac{\pi x}{l} \quad (4.7)$$

with $\frac{B}{A} = \frac{\psi d}{2D}$ for elastically restraint edges.

a. Edges $y = \pm\frac{d}{2}$ hinged (B = o)

For

$$\frac{l}{d} = \sqrt[4]{\frac{E_{tx}}{E_{ty}}} \quad (4.8)$$

a minimum value of σ_{cr} is obtained,

$$\sigma_{cr} = \frac{\pi^2}{12}\left(\frac{w}{d}\right)^2 \left[\frac{2\sqrt{E_{tx}E_{ty}} + \nu_y E_{tx} + \nu_x E_{ty}}{1-\nu_x\nu_y} + 4G_t\right] \quad (4.9)$$

b. Edges $y = \frac{d}{2}$ completely fixed ($A = 0$)

For

$$\frac{l}{d} = 0.66\sqrt[4]{\frac{E_{tx}}{E_{ty}}} \quad (4.10)$$

a minimum value of σ_{cr} is obtained

$$\sigma_{cr} = \frac{\pi^2}{12}\left(\frac{w}{d}\right)^2 \left[\frac{4.554\sqrt{E_{tx}E_{ty}} + 1.237(\nu_y E_{tx} + \nu_x E_{ty})}{1-\nu_x\nu_y} + 4.948\,G_t\right] \quad (4.11)$$

5. Determination of G_t at Strain Hardening from Results of Angle Tests

The critical stress for torsional buckling of angles is given by equation (4.3).

Figures 4 and 5 of Progress Report T show that angle specimens A-31, A-32, and A-33 failed due to torsional buckling at about the point of strain hardening. Coupon tests gave an average value of E_{tx} at strain hardening of about E_{ts} = 900 ksi

With assumed values of ν_x and ν_y, G_{ts} can be computed from Eq. (4.3)

a. Annealed material (Tests A-31, A-32)

$\sigma_{cr} = 35$ ksi, $\frac{b}{t} = 8.8$, $\frac{l}{b} = 2.74$:

- $\nu_x = \nu_y = 0.5$ $\quad G_{ts} = 2{,}580$ ksi
- $\nu_x = 0.5$ $\nu_y = 1.0$ $\quad G_{ts} = 2{,}510$ ksi

b. As-delivered material (Test A-33)

$\sigma_{cr} = 45$ ksi, $\frac{b}{t} = 8.7$, $\frac{l}{b} = 2.65$:

- $\nu_x = \nu_y = 0.5$ $\quad G_{ts} = 3{,}270$ ksi
- $\nu_x = 0.5$ $\nu_y = 1.0$ $\quad G_{ts} = 3{,}210$ ksi

From the general expressions summarized in Table I numerical values of E_{tx}, E_{xy}, G_t, ν_x and ν_y are computed for the beginning of the strain-hardening range taking

$$E_{ts} = 900 \text{ ksi}$$

$$E = 30{,}000 \text{ ksi}$$

$$\text{and } \nu = 0.3$$

$$\text{or } \nu = 0.5$$

The results are summarized in Table II. The most important factor for the buckling strength of outstanding flanges is G_t. It is seen that Bleich's semi-rational theory comes closest to the above computed values.

6. Tests on Wide-Flange Sections

In order to investigate the actual behavior of WF shapes with regard to local buckling 6 shapes were tested under two extreme loading conditions:

1° axial compression (Test D1,D2,D3,D4,D5,D6)

2° pure bending (Test B1, B2, B3, B4, B5, B6)

The test set-ups for both kinds of tests are shown in Fig. 6.1. The length of each specimen was divided into three gage lengths over which the change in length was measured directly with 0.0001" Ames dials. Along the edges of the flanges and the center of the web deflection measurements were taken as shown in the same figure. For the bending tests [redacted] the lateral rotation was measured at the loading points (which were supported against lateral rotation) and near the center line of the beam. The dimensions of all specimens are given in Table III.

Fig. 6.2 shows the obtained P/A vs ε_{av} curves from the compression tests and M/Z vs ε_{av} curves from the bending tests (ε_{av} = average strain at center of compressed flange)

A = area of cross-section

Z = plastic section modulus

For all tests curves giving maximum flange deflection, maximum web deflection and lateral rotation vs average strain were plotted. A typical example is given in Fig. 6.3 (Tests D2, B2). From these curves the critical strains were obtained. The critical strain is defined as the strain at which the lateral deflection of flange or web starts to increase more rapidly. Figs. 6.4 and 6.5 show the strain distribution along the length of specimens together with flange deflections, web deflections and lateral rotation.

The results are summarized in Table IV. The critical strains of the flanges are plotted vs the b/t ratio in Fig. 6.6, showing also the corresponding theoretical curves.

Specimens D4 and D5 failed primarily due to web buckling and these two results are plotted in Fig. 6.7 as a function of d/w. The result of test D2 is also plotted in the same figure.

List of References

1. Thürlimann, B., Haaijer, G., "Buckling of Steel Angles in the Plastic Range", Progress Report T, Fritz Laboratory, Lehigh University, August, 1953.

2. Haaijer, G., "Compression Tests on Short Steel Columns of Rectangular Cross-Section", Progress Report S, Fritz Laboratory, Lehigh University, June, 1953.

3. Girkmann, K., "Flächentragwerke", 2nd Edition Springer-Verlag, Vienna, 1948.

4. Bleich, F., "Buckling Strength of Metal Structures", McGraw-Hill, New York, 1952.

5. Lundquist, E.E., Stowell, E.Z., "Critical Compressive Stress for Outstanding Flanges", N.A.C.A., Report No. 734, 1942.

6. Lundquist, E.E., Stowell, E.Z., "Critical Compressive Stress for Flat Rectangular Plates Supported Along all Edges and Elastically Restrained Against Rotation Along the Unloaded Edges", N.A.C.A. Report No. 733, 1942.

7. Kaufmann, W., "Bemerkungen zur Stabilität Dünnwandiger Kreiszylindrischer Schalen Oberhalb der Proportionalitäts Grenze", Ingenier-Archiv, 1935, Vol. VI No. 6.

8. Bijlaard, P.P., "Some Contributions to the Theory of Elastic and Plastic Stability", Pubs. Intern. Assoc. for Bridge and Structural Engineering, Vol. VIII, 1947.

9. Ilyushin, A.A., "Stability of Plates and Shells Beyond the Proportional Limit", NACA TM-1116, October, 1947.

10. Stowell, E.Z., "A Unified Theory of Plastic Buckling of Columns and Plates", N.A.C.A. Report 898, 1948

11. Handleman, G.H., Prager, W., "Plastic Buckling of a Rectangular Plate with Edge Thrust", N.A.C.A. TN-1530, 1948.

TABLE I

Theory		E_{tx}	E_{ty}	G_t	ν_x	ν_y
Bleich	(Ref. 4)	E_t	E	$\frac{\sqrt{E\ E_t}}{2(1+\nu)}$	$\nu\sqrt{\frac{E_t}{E}}$	$\nu\sqrt{\frac{E}{E_t}}$
Kaufmann	(Ref. 7)	E_t	E	$\frac{E\ E_t}{(1+\nu)(E+E_t)}$	ν	ν
Bijlaard Ilyushin Stowell	(Ref. 8) (Ref. 9) (Ref.10)	E_t	$\frac{E_t}{\frac{1}{4}+\frac{3}{4}\frac{E_t}{E_{sec}}}$	$\frac{E_{sec}}{3}$	$\frac{1}{2}$	$\frac{1}{\frac{1}{2}+\frac{3}{2}\frac{E_t}{E_{sec}}}$
Handelmann Prager	(Ref.11)	E_t	$\frac{4EE_t}{E+3E_t}$	$\frac{E}{2(1+\nu)}$	$\frac{E_t(2\nu-1)+E}{2E}$	$\frac{2[E_t(2\nu-1)+E]}{E+3E_t}$

TABLE II

Theory		E_{tx} ksi	E_{ty} ksi	G_t ksi	ν_x	ν_y
Bleich	$\nu = 0.5$	900	30,000	1,730	0.09	2.39
	$\nu = 0.3$	900	30,000	2,000	0.05	1.73
Kaufmann	$\nu = 0.5$	900	30,000	580	0.5	0.5
	$\nu = 0.3$	900	30,000	670	0.3	0.3
Bijlaard Ilyushin Stowell	$\sigma_y = 35$ ksi, $\epsilon_s = 13x10^{-3}$	900	1,760	860	0.5	0.98
	$\sigma_y = 45$ ksi, $\epsilon_s = 13x10^{-3}$	900	2,000	1,110	0.5	1.10
Handelman Prager	$\nu = 0.3$	900	3,300	11,500	0.49	1.82

TABLE III

Dimensions of Specimens

Spec.	Shape	A in^2	Z in^3	b in	t in	d in	w in	L in	L^1 in	C in	B/t	b/t	d^*/w
B1 D1	10 WF 33	9.66	38.56	7.95	0.429	9.80	0.294	32	32	38	18.5	9.2	30.4
B2 D2	8 WF 24	6.83	22.56	6.55	0.383	8.01	0.236	26	26	38	17.1	8.6	30.7
B3 D3	10 WF 39	11.34	45.63	8.02	0.512	9.88	0.328	32	32	48	15.6	7.8	27.0
B4 D4	12 WF 50	14.25	70.28	8.18	0.620	12.19	0.351	32	32	52	13.2	6.6	31.2
B5 D5	8 WF 35	10.00	33.68	8.08	0.476	8.13	0.308	32	32	44	17.0	8.5	23.3
B6 D6	10 WF 21	5.84	22.45	5.77	0.318	9.82	0.232	23	26	30	18.2	9.1	39.6

$d^* = d - 2t$

TABLE IV

Test Results

Test	σ_y ksi	$\epsilon_{cr} \times 10^3$		σ_{cr} ksi	
		Flange	Web	Flange	Web
D 1	34.4	8.5	8.5	34.2	34.2
D 2	34.0	13.5	13.0	34.0	34.0
D 3	35.2	17.5	17.5	38.5	38.5
D 4	35.0	18.5	6.0	36.8	35.2
D 5	36.6	15.0	15.0	37.7	37.7
D 6	38.0	4.3	1.6	33.8	38.0
B 1		7.0			
B 2		23.0			
B 3		22.5			
B 4		27.5			
B 5		20.5			
B 6		14.0			

Bending Test

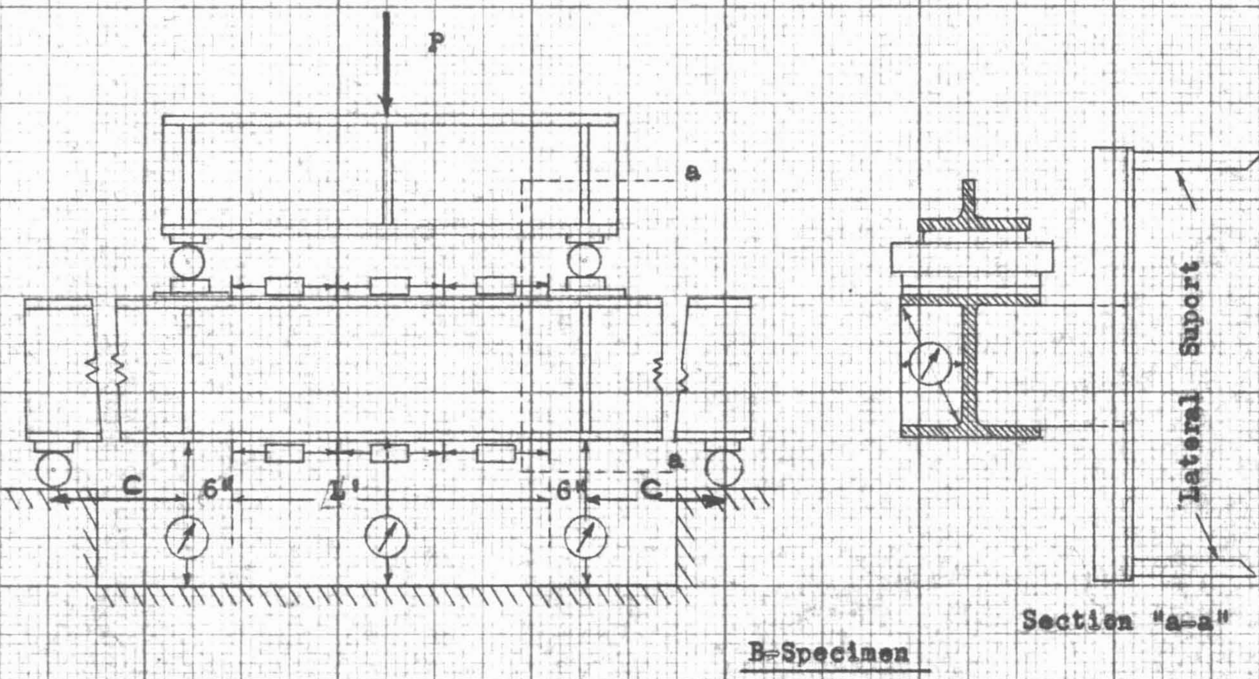

Compression Test

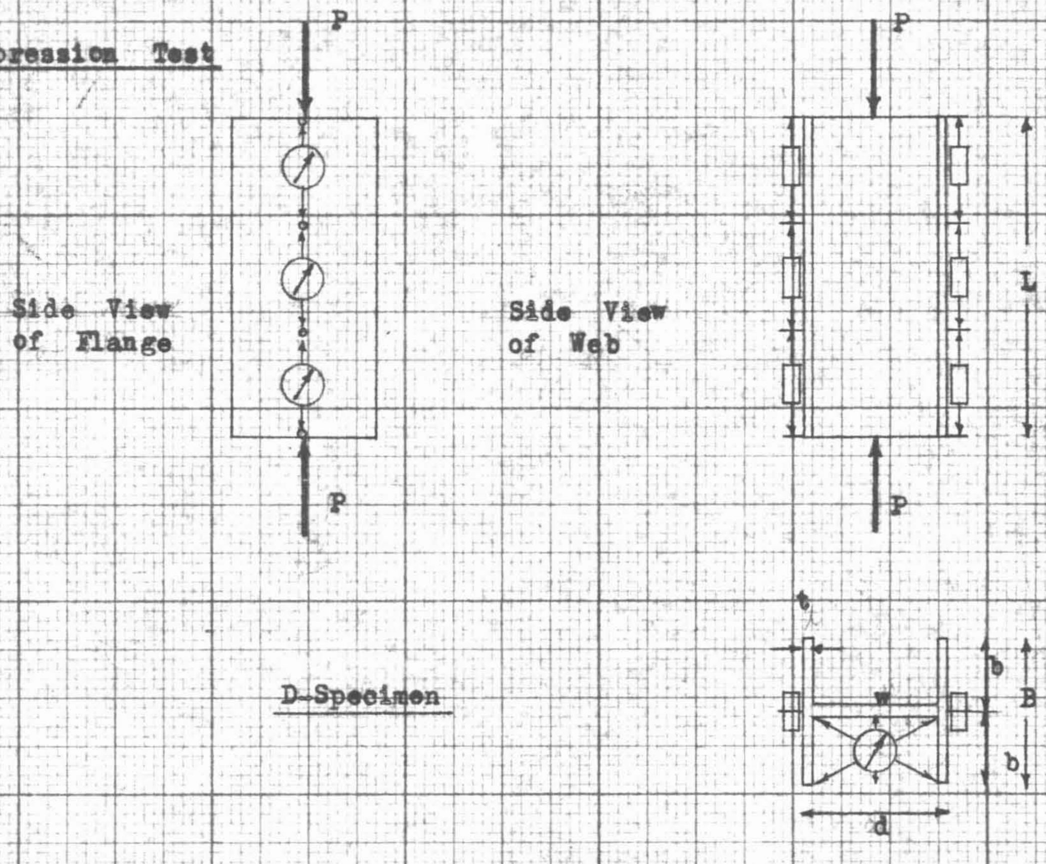

Fig. 6.1 Test Set-ups

205E-4

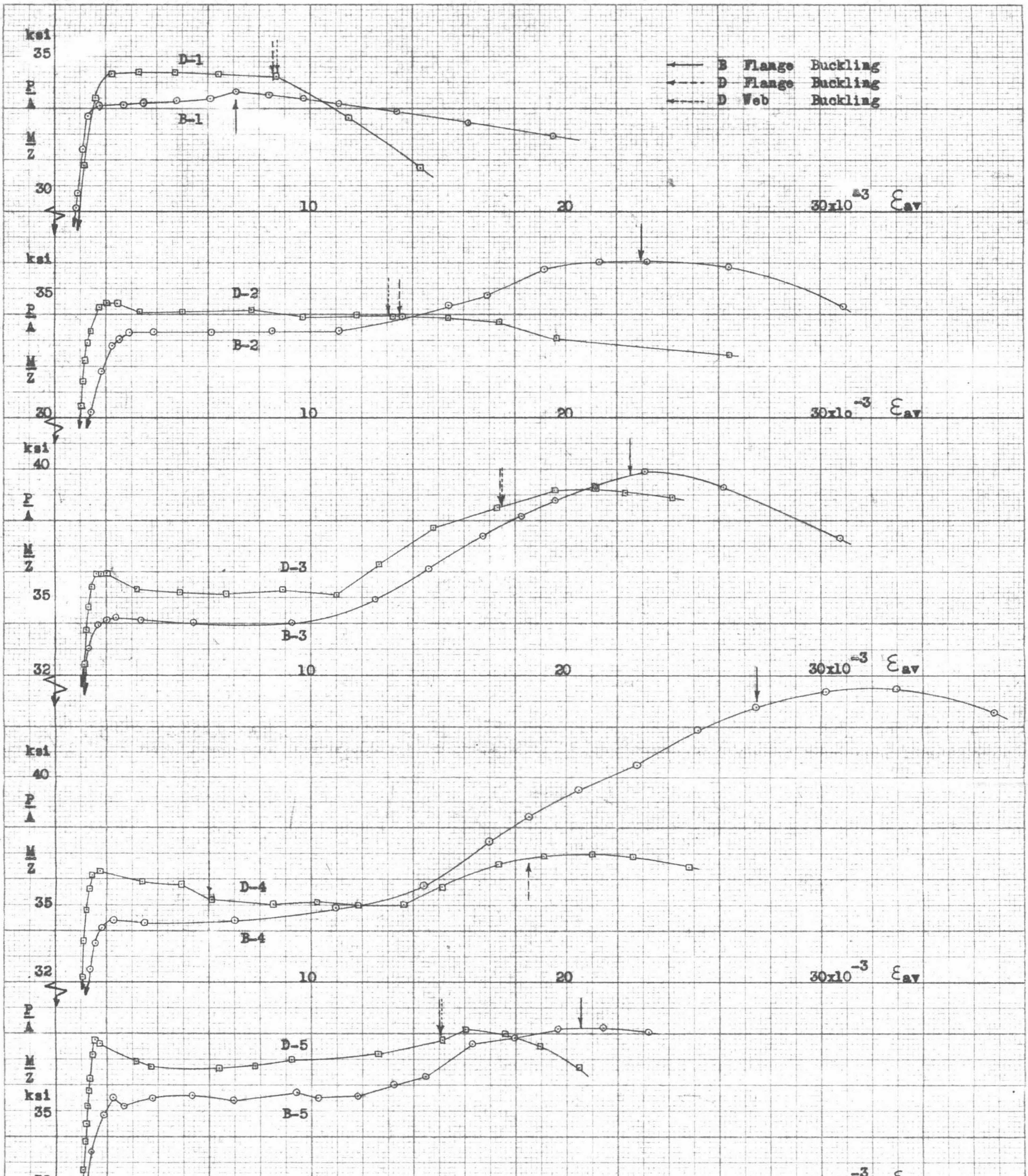

Fig. 6-2 P/A vs ε_{av} and M/Z vs ε_{av} curves

205E-4

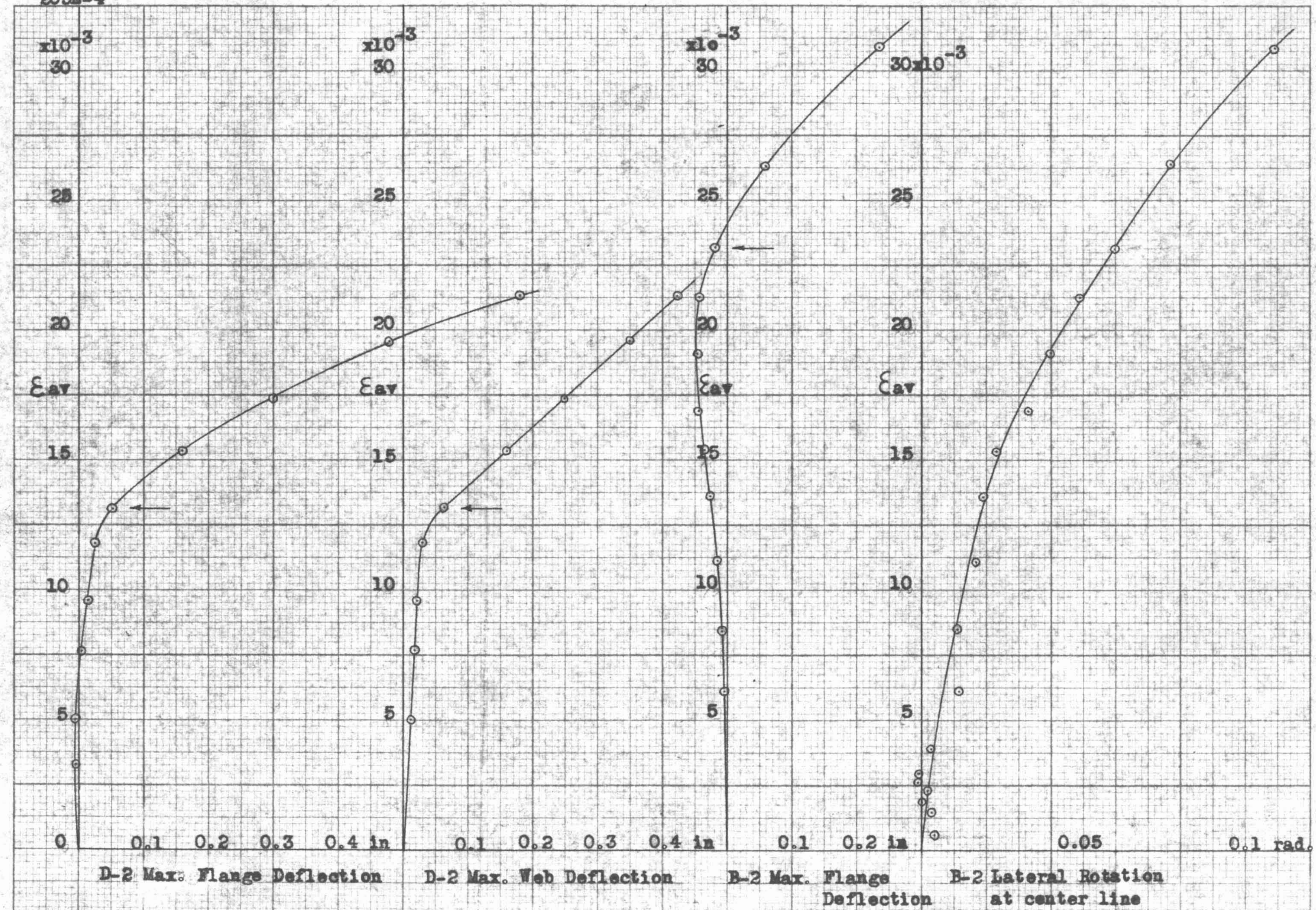

Fig. 6.3 Flange-Deflection, Web-Deflection and Lateral-Rotation vs Average Strain Curves

205E-4

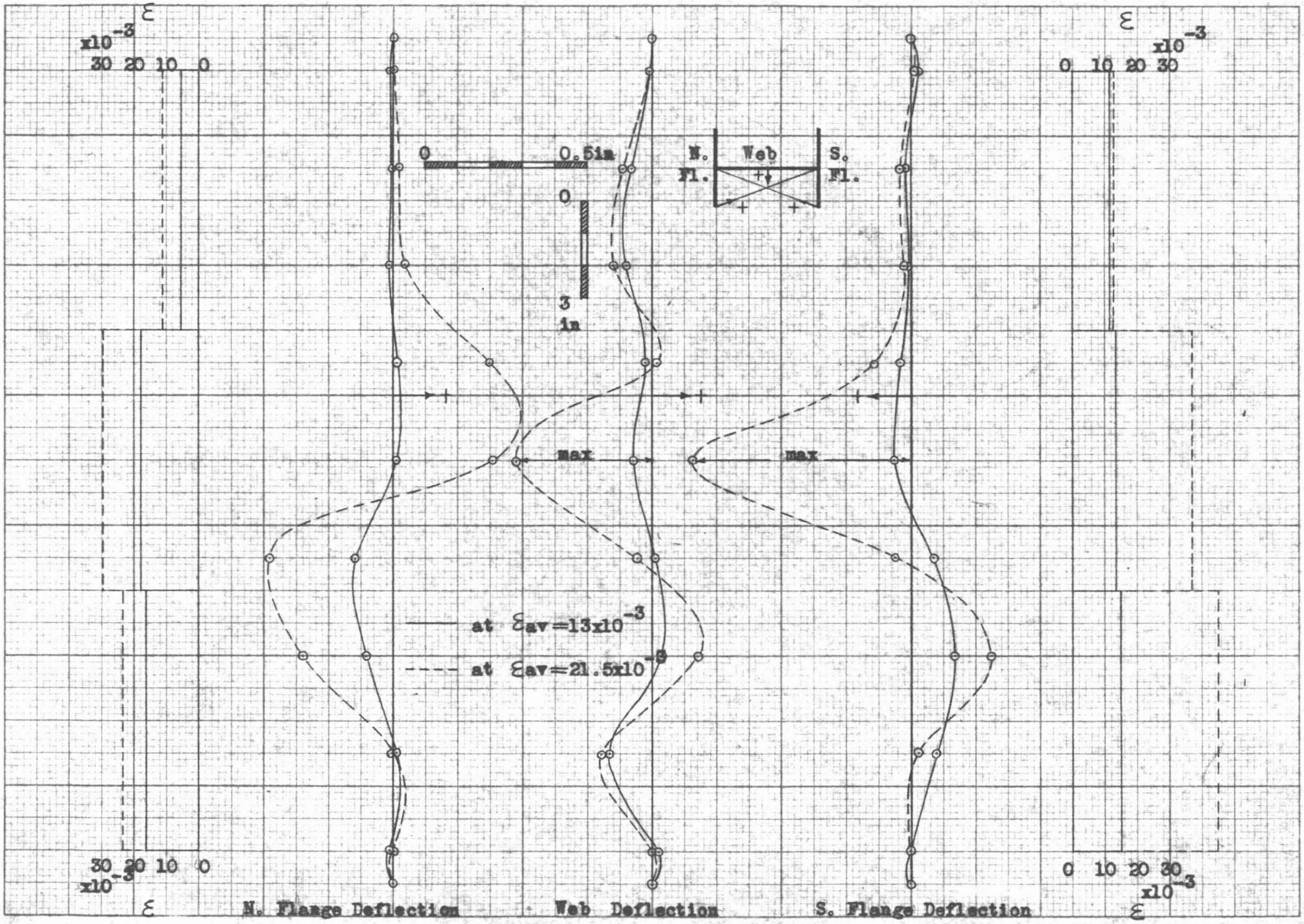

Fig. 6.4 Flange and Web Deflection of Specimen D-2

205E-4

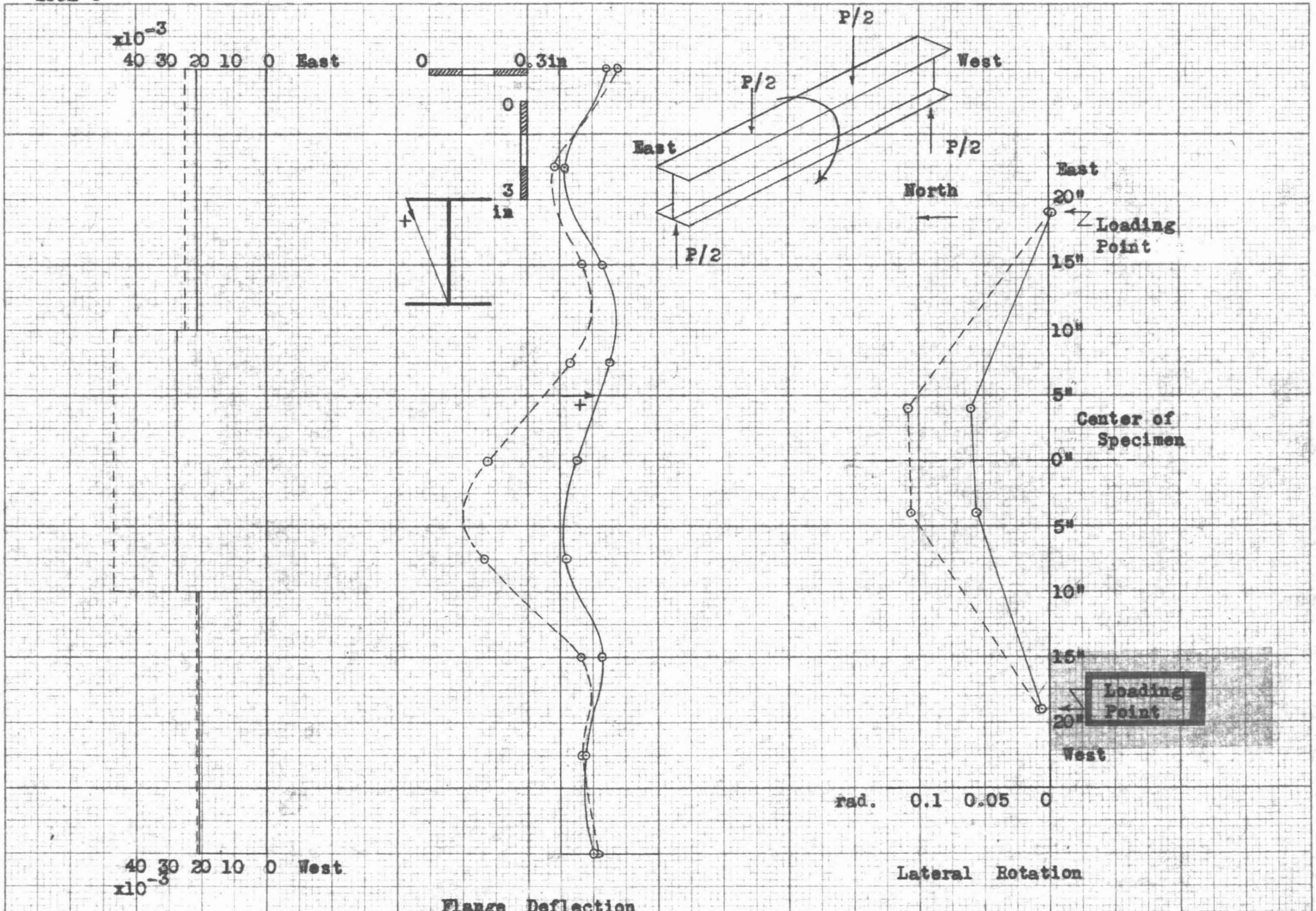

Fig. 6.5 Flange-Deflection and Lateral-Rotation of Specimen B-2

205E-4

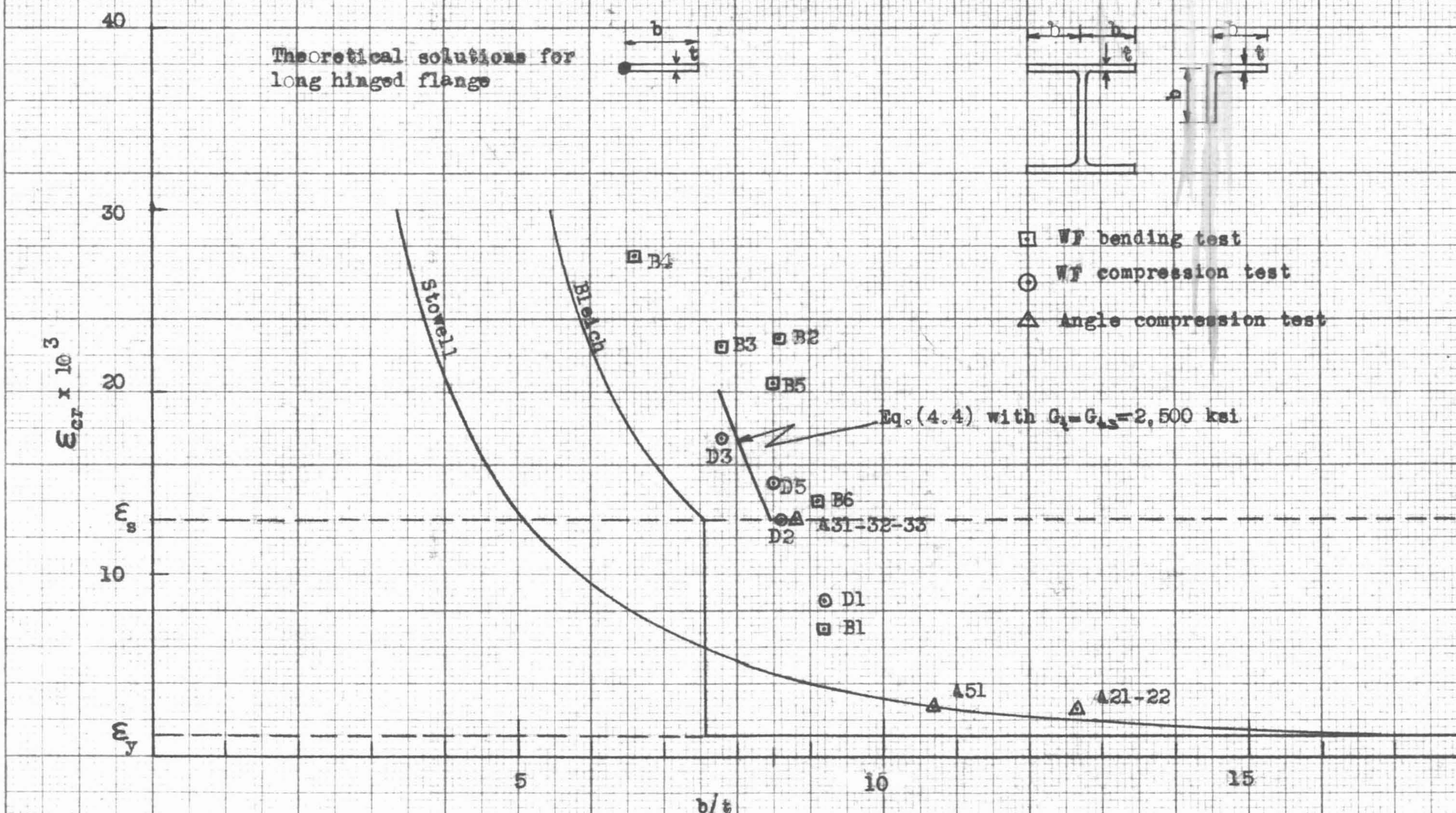

Fig. 6.6 Flange Buckling

205E-4

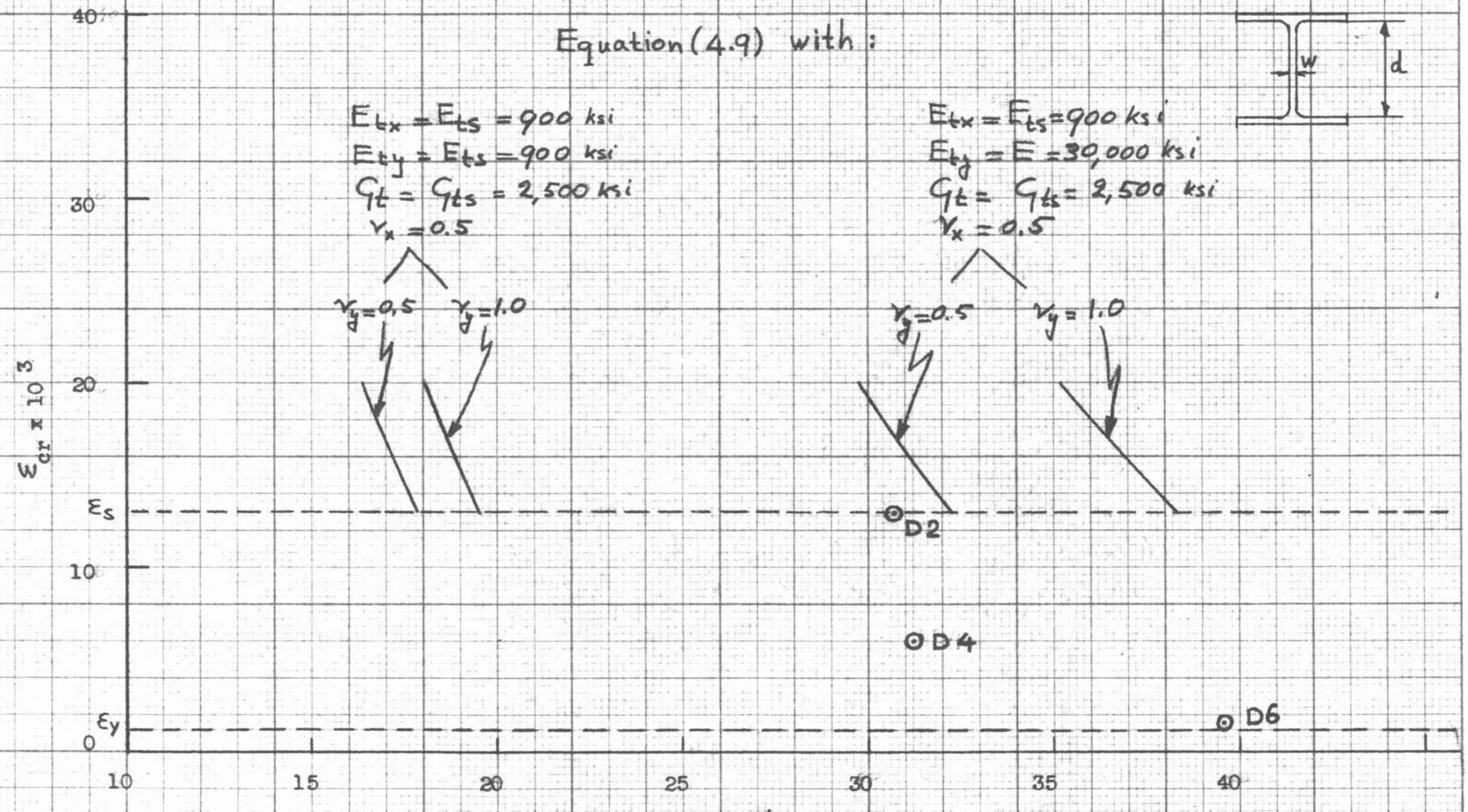

Fig. 6.7 Web Buckling